MORC3, a component of PML Nuclear Bodies, has a role in restricting herpes simplex virus type 1 and human cytomegalovirus

Elizabeth Sloan[#], Anne Orr and Roger D. Everett

MRC-University of Glasgow Centre for Virus Research
Garscube Campus, 464 Bearsden Road, Glasgow G61 1QH
Scotland, U.K.

corresponding author
elizabeth.sloan@glasgow.ac.uk
Tel: + 44 141 330 3922
Fax: + 44 141 330 3520

Running title: Restriction of HSV-1 and HCMV by MORC3

Key words: MORC3, PML, ICP0, SUMO, HSV-1, HCMV

Abstract word count: 233
Main text word count: 5168

ABSTRACT

We previously reported that MORC3, a protein associated with promyelocytic leukemia nuclear bodies (PML NBs), is a target of HSV-1 ICP0 mediated degradation. Since it is well known that certain other components of the PML NB complex play an important role during an intrinsic immune response to HSV-1, and are also degraded or inactivated by ICP0, we further investigate here the role of MORC3 during HSV-1 infection. We demonstrate that MORC3 has antiviral activity during HSV-1 infection and that this antiviral role is counteracted by ICP0. In addition, MORC3's antiviral role extends to wild type (wt) HCMV infection as its plaque forming efficiency increased in MORC3 depleted cells. We found that MORC3 is recruited to sites associated with HSV-1 genomes after their entry into the nucleus of an infected cell, and in wt infections this is followed by its association with ICP0 foci prior to its degradation. The RING finger domain of ICP0 was required for degradation of MORC3 and we confirmed that no other HSV-1 protein is required for the loss of MORC3. We also found that MORC3 is required for fully efficient recruitment of PML, Sp100, hDaxx and γH2AX to sites associated with HSV-1 genomes entering the host cell nucleus. This study further unravels the intricate ways in which HSV-1 has evolved to counteract the host immune response and reveals a novel function for MORC3 during the host intrinsic immune response.

IMPORTANCE

Herpesviruses have devised ways to manipulate the host intrinsic immune response to promote their own survival and persistence within the human population. One way in which this is achieved is through degradation or functional inactivation of PML nuclear body (PML NB) proteins which are recruited to viral genomes in order to repress viral transcription. Because MORC3 associates with PML NBs in uninfected cells, and is a target for HSV-1 mediated degradation, we investigated the role of MORC3 during HSV-1 infection. We found that MORC3 is also recruited to viral HSV-1 genomes and importantly it contributes to the fully efficient recruitment of PML, hDaxx, Sp100 and γH2AX to these sites. Depletion of MORC3 resulted in an increase in ICP0-null HSV-1 and wt HCMV replication and plaque formation, and therefore this study reveals that MORC3 is an antiviral factor which plays an important role during HSV-1 and HCMV infection.

INTRODUCTION

Herpes simplex virus 1 (HSV-1) is endemic in populations throughout the world and responsible for a number of clinically important diseases that range from facial and genital lesions to encephalitis (1, 2). This alpha herpesvirus establishes lifelong persistence within the host, remaining latent within sensory ganglia after the primary infection is resolved. Periodically the virus is reactivated from its latent state resulting in recurrent lesions. HSV-1 has the capacity to remain persistent within the host and allow transmission within the population due to a variety of immune evasion strategies which it encodes.

Upon initial infection there is activation of an intrinsic immune response involving constitutively expressed proteins such as the promyelocytic leukaemia (PML) protein and other components of the PML nuclear body (PML NB) complex (e.g. Sp100 and hDaxx), which restrict viral gene replication (3-6). Wild-type (wt) HSV-1 overcomes this aspect of restriction though expression of the viral ubiquitin E3 ligase protein, ICP0, that preferentially targets specific SUMO (small ubiquitin-like modifier) modified proteins for proteasome-mediated degradation. These include PML and certain other components of the PML NB complex (7, 8). In addition to these PML NB associated proteins, HSV-1 infection results in an extensive reduction of high molecular weight SUMO-conjugated proteins at late times of infection. We recently used SILAC proteomics and mass spectrometry to identify a number of these SUMO2-modified proteins whose abundance is altered during HSV-1 infection (9). MORC3 (microrchidia family CW-type zinc-finger 3, also known as NXP-2) was one such sumoylated protein which we discovered was decrease in abundance by 5.6 fold during HSV-1 infection. We went on to confirm that MORC3 was indeed sumoylated and that both sumoylated and unmodified forms were degraded during HSV-1 infection in an ICP0-dependent manner (9).

MORC3 is a nuclear matrix protein whose functional domains are highly conserved between prokaryotes and eukaryotes (10, 11), however the function of MORC3 has not been studied in great detail. Interestingly, previous reports showed that MORC3 can associate with PML NBs (12). The localization of MORC3 to PML NBs is dependent on a SUMO-SIM (SUMO Interaction Motif) interaction with PML isoform I (PML.I) (13). In addition, Takahashi and colleagues found that Sp100 and p53 were recruited to PML NBs in a MORC3- dependent manner, providing some insight into the function of MORC3 within these complexes. MORC3 was also found to form nuclear body complexes in a PML-

independent manner after transient over-expression, with the function of these structures unknown (13).

In humans there are five members of the MORC family; MORC1-4 and the divergent SMCHD1 protein (structural maintenance of chromosome flexible hinge domain containing 1). There are three conserved domains within MORC3; the GHL (gyrase B, Hsp90, and MutL) ATPase domain (14), a CW-type zinc finger domain (15), and a coiled-coil dimerization domain (16, 17). The GHL-ATPase domain is thought to be involved in gene silencing and regulation of chromatin structure in response to DNA damage signals (18-20), and is required for localization of MORC3 to PML NBs and the recruitment of Sp100 and p53 to these structures (12). The CW-type zinc finger domain contains a histone H3 binding motif which binds predominantly methylated lysine 4 of histone H3 (21-23). The function of the coiled-coil domain within MORC proteins is unknown, although this domain in other proteins has been suggested to regulate protein-protein and protein-DNA interactions, protein localization, gene transcription, the DNA damage response and signal transduction (24-43).

It has been suggested, therefore, that MORC3 is an epigenetic regulator that may play roles within a wide range of biological functions such as transcription regulation, chromatin condensation and remodeling, and DNA break repair (44). Members of the MORC family of proteins have been associated with a number of types of cancers (45-49). However, to date there is little known about the role that MORC3 may play during a virus infection, although one recent study reported that MORC3 is required for efficient influenza replication (50). Until now, MORC3 has not been previously reported to have an antiviral role. Following our discovery that sumoylated MORC3 is targeted by ICP0 (9), we examined here the function of MORC3 during infection with HSV-1 and found that it is efficiently recruited to incoming HSV-1 genomes at early times post infection. We also discovered that during ICP0-null mutant infection of MORC3 depleted cells the recruitment of Sp100, hDaxx, PML and γH2AX to incoming viral genomes were less efficient. In addition, we observed that MORC3 colocalized with ICP0 early during infection, prior to its degradation in a RING-finger dependent manner. Importantly, MORC3 was found to have antiviral activity which is counteracted in the presence of ICP0, and that MORC3 restricts wt human cytomegalovirus (HCMV) plaque formation efficiency, suggesting that MORC3 has an antiviral role that extends beyond HSV-1.

MATERIALS AND METHODS

Viruses and cells. HSV-1 wild type (wt) strain 17+ was used, from which the ICP0 null mutant *dl*1403 was derived (51). Wild type HSV-1, *in*1863, and the derivative *dl*1403/CMV*lac*Z, both contain the *lac*Z gene under the control of the HCMV promoter/enhancer inserted into the *tk* gene and were gifts from Chris Preston. HSV-1 *dl*0Y4 expresses EYFP-linked ICP4 and was derived from *dl*1403 (52). Viruses were propagated in Baby Hamster kidney (BHK) cells grown in Glasgow modified Eagles' medium (Gibco Life Technologies) supplemented with 10% newborn calf serum (Gibco Life Technologies) and 10% tryptose phosphate broth (Gibco Life Technologies). Virus titres were determined by titration on U2OS cells in the presence of 1% human serum (MP Biomedicals). Viral plaques were visualized using Geimsa stain (VWR). Human foreskin diploid human fibroblasts (HFs, a gift from Thomas Stamminger), telomerase-immortalized HFs (HFTs, a gift from Chris Boutell), HEK-293T cells and U2OS cells were all grown in Dulbecco's modified Eagles' medium (Gibco Life Technologies) supplemented with 10% fetal bovine serum (FBS) (Gibco Life Technologies), 100 units/ml penicillin and 0.1 mg/ml streptomycin (Gibco Life Technologies). HepaRG cells (53), were grown in William's medium E (Gibco Life Technologies) supplemented with 10% FBS, 2 mM glutamine (Gibco Life Technologies), 5 µg/ml insulin (Sigma-Aldrich), and 500 nM hydrocortisone (Sigma-Aldrich). HepaRG cells that can be induced to express ICP0 (HA-cICP0), or ICP0 mutants (HA-FXE, HA-mSLS4, HA-mSLS457, HA-E52X) in the presence of doxycycline (0.1 µg/ml) (Clontech) were described previously (7, 54). Lentivirus transduced cells were maintained with the appropriate antibiotic selection.

Plasmids and lentiviral vectors. Lentivirus vectors expressing anti-MORC3 shRNA (shMORC3) were obtained from Sigma-Aldrich (shMORC3-1335**:**CCGGGCTTAATACGT GTCGGTCATACTCGAGTATGACCG ACACGTATTAAGCTTTTT), (shMORC3-1337: CCGGGCCAATTACAAGAACTGAGAACTCGAGTTCTCAGTTCTTGTAATTGGCTTT TT), (shMORC3-1339: CCGGGTGAGGTTGAATTGCTGGAAACTCGAGTTTCCAGCA ATTCAACCTCACTTTTT). Lentivirus transduction of cells was as described previously (55). Briefly, pLKO plasmids expressing the gene of interest were cotransfected along with pVSV-G and pCMV.DR.8.91 (a gift from Didier Trono) into HEK-293T cells. Lentivirus supernatants were collected and HFT and HepaRG cells transduced. Selection during routine culture used puromycin at 500 ng/ml, which were omitted from cells seeded for and during experimentation. HA-cICP0 cells and their derivatives were maintained in media containing G418 (500 µg/ml) and puromycin.

Virus plaque assays. The relative plaque forming efficiencies of wt and ICP0 null mutant HSV-1 were assessed as described (56), with HFT-shMORC3 cells seeded for plaque assays into 24-well dishes at 1 x 10^5 cells per well, and infected the following day with appropriate sequential 3-fold dilutions of *dl*1403/CMV*lac*Z or wt *in*1863. After virus adsorption, the cells were overlayed with medium containing 1% human serum. The cells were then stained for β-galactosidase positive plaques 24 h later. Relative plaque formation efficiencies are expressed as fold changes in plaque numbers at a given dilution compared to the control. This approach gives a more robust and reliable comparison compared to apparent titres averaged over a range of dilutions because the plaque forming efficiency of ICP0 null mutant HSV-1 varies in a non-linear manner with respect to dilution. For assay of HCMV plaque formation, HFT-shMORC3 and control cells were seeded into 24-well dishes and infected with HCMV at appropriate multiplicities the following day. At 3 h after virus adsorption, the virus inoculum was removed and replaced with fresh medium. Plaques were stained at 10 days after infection by immunological detection of UL44 (ab6502, Abcam). The cells were fixed with formaldehyde and treated with NP40 as for immunofluorescence staining, then washed twice with phosphate-buffered saline (PBS) containing 0.1% Tween-20 (PBST). The cells were treated with PBST containing 5% dried milk for 30 minutes and then incubated for 2 h at room temperature with anti-UL44 monoclonal antibody. The cells were then washed three times with PBST before being incubated with horse radish peroxidase (HRP) conjugated goat anti-mouse secondary antibody for 1 h. The cells were washed with PBST three times and incubated with 0.2 ml True Blue solution (50-7802, Insight Biotechnology) for 10 minutes.

Western blot analysis. Cells were seeded into 24-well dishes at 1 x 10^5 cells per well. After the relevant experimental manipulations, the cells were washed twice with PBS before harvesting in sodium dodecyl sulfate-polyacrylamide gel electrophoresis (SDS-PAGE) loading buffer. Proteins were resolved on 7.5% SDS-PAGE and then transferred to nitrocellulose membranes by western blotting. The following primary antibodies were used: anti-actin mAb (AC-40) (Sigma-Aldrich) (1:10,000), anti-PML mAb (5E10) (57) (1:100), anti-tubulin mAb (T4026) (Sigma-Aldrich) (1:5000), anti-ICP0 mAb (11060) (58) (1:1000), anti-ICP4 mAb (58S) (59) (1:1000), anti-UL42 mAb (Z1F11) (60) (1:1000), anti-Sp100 rAb (SpGH) (61) (1:2000), anti-MORC3 rAb (NBP1-83036) (Novus Biologicals) (1:300), anti-RanGAP1 mAb (33-0800) (Invitrogen) (1:1000). Secondary antibodies included: anti-mouse-

HRP (A4416) (Sigma-Aldrich) (1:1500), anti-Rabbit-HRP (A4914) (Sigma-Aldrich) (1:20,000).

Immunofluorescence and confocal microscopy. Cells were seeded onto 13 mm glass coverslips within 24-well plates at 1 x 10^5 cells per well, fixed and prepared for immunofluorescence as described (62). Antibodies used were: anti-PML mAb (5E10) (57) (1:20), anti-Sp100 rat serum (Sp26) (63) (1:2000), anti-MORC3 rAb (NBP1-83036) (Novus Biologicals) (1:400), anti-ICP0 mAb (11060) (58) (1:1000), anti-hDaxx mAb (MCA2143) (AbD Serotech) (1:1000), anti-Phospho-H2AX (Ser139) rAb (clone JBW301-Upstate) (1:1000) and nuclei were stained with DAPI (Sigma-Aldrich). The secondary antibodies used were Alexa 555 conjugated goat anti-mouse IgG (Life Technologies) (1:5000), Alexa 633 conjugated goat anti-rabbit IgG (Life Technologies) (1:1000), Alexa 488 conjugated goat anti-mouse IgG (Life Technologies) (1:1000), Alexa 488 conjugated goat anti-rat IgG (Life Technologies) (1:1000) and Alexa 555 conjugated goat anti-rat IgG (Life Technologies) (1:5000). Immunofluorescence assays were done in replicate and complete coverslips were examined in detail using a Zeiss LSM 710 confocal microscope, with 488 nm, 561 nm and 633 nm laser lines, scanning each channel separately under image capture conditions that eliminated channel overlap.

RESULTS

MORC3 colocalizes with ICP0 prior to its degradation. MORC3 can be detected within PML NBs and in one reported instance was found to be required for recruitment of Sp100 into these nuclear complexes (12, 13). Our study also observed MORC3 in association with PML NBs, although following examination of a large number of cells we noted that not every PML NB complex had detectable MORC3 (Fig. 1, see also Figs. 4 and 5 below). This difference may be due to differences in cell types analyzed and methods used, or a limit of antibody detection efficiency. At the early stages of HSV-1 infection, ICP0 colocalizes with PML NB protein components such as PML and Sp100 prior to their degradation (8, 64-67). Since we have previously shown that both sumoylated and unmodified MORC3 is degraded during wt HSV-1 infection (9), we investigated whether MORC3 also colocalizes with ICP0 prior to its degradation. Human diploid fibroblasts (HFs) were infected for 1 h with wt HSV-1 at multiplicity of infection (MOI) of 2 plaque forming units (pfu) per cell. The localization of ICP0 and MORC3 were then visualized using immunofluorescence staining and confocal microscopy, with mock infected cells included as a control (Fig. 1). Complete coverslips were examined of which 21 and 38 cells were imaged at 1 and 2 h p.i, respectively. We found

that by 1 h after wt HSV-1 infection MORC3 colocalizes with ICP0 (cell indicated with arrow), prior to loss of the MORC3 signal in cells where ICP0 expression is more intense. By 2 h post infection all cells expressing ICP0 contained no detectable MORC3 protein, with MORC3 only found in uninfected cells within this population. Some colocalization of MORC3 with an ICP0 RING-finger mutant was also observed (data not shown), suggesting this association is independent of the RING finger domain of ICP0. Therefore, MORC3 colocalizes with ICP0 very early during infection prior to its degradation.

MORC3 is degraded in an ICP0 dependent manner during HSV-1 infection. Our previous study found that ICP0 expressed on its own is sufficient to cause a reduction in MORC3 protein abundance (9). However, it remains possible that other HSV-1 proteins display similar activity. Therefore, to confirm that no other HSV-1 proteins are capable of causing the degradation of MORC3 we infected telomerase-immortalized HFs, with ICP0-null mutant HSV-1(MOI 20) over a time course infection, with wt HSV-1 (MOI 2) included as a control. The different multiplicities of wt and mutant were used to enable similar rates of infection progression. Western blot analysis indeed confirmed that wt but not ICP0-null mutant HSV-1 infection results in a loss of MORC3 (Fig. 2). Therefore, we have shown through expression of ICP0 alone (9), and infection with an ICP0-null HSV-1, that ICP0 is the only HSV-1 protein required for the observed reduction in MORC3.

The RING finger domain of ICP0 is required for MORC3 degradation. The region of ICP0 required for the degradation of MORC3 was assessed by utilizing cells that can be induced to express wt or mutant forms of ICP0 (54, 68). In this study we utilized mutants of ICP0 that lack the RING finger domain, one or more of the motifs resembling SIMs termed SIM-like sequences (SLS1-7) and a C-terminal deletion (Fig. 3A). Each region has individually been shown to be involved in the efficiency of degradation of selected proteins. The RING finger domain functions as a ubiquitin ligase which is required for degradation of many proteins including unsumoylated PML.I, while the SLS motifs are likely to influence target specificity of the RING finger activity by binding to SUMO moieties which are conjugated to sumoylated proteins. We have found that the SLS4 motif is involved in targeting specific sumoylated proteins including NACC1, ZBTB10, ZBTB4, ETV6 and specific PML isoforms (7, 9, 69) and data not shown). However the SLS4 motif was not required for degradation of other sumoylated proteins such as MBD1, BEND3, ZBTB12, NACC2 or ARID3a (9) and data not shown), demonstrating there is specificity in the SLS4-targeted group of proteins. A combination of mutations within these SLS motifs (mSLS457) diminishes ICP0 function and reduces the rate at which it causes the extensive reduction in

high molecular weight SUMO conjugates (7). There are also motifs within the C-terminal region of ICP0 that have been implicated in binding to other proteins (70-72). To identify the regions of ICP0 that are involved in the degradation of MORC3, cells were induced to express either full length ICP0, ICP0 RING finger deletion (FXE), ICP0 C-terminal deletion (E52X), ICP0 with a mutation in the SLS4 motif (mSLS4) or a combination of mutations in SLS4, 5 and 7 (mSLS457). Western blot analysis of these cell lysates prepared with or without ICP0 induction included PML as a control (Fig. 3B). As expected from previous results, expression of wt ICP0 and mutants E52X and mSLS4 caused substantial degradation of PML (7). The reduction in the PML band intensity in the RING finger mutant FXE sample in this particular gel was not reproducible and was not observed in a number of previous published reports (for example (54)) and therefore we regard this as spurious. Degradation of sumoylated PML isoforms is evident in the cells expressing ICP0 mutant SLS457, which is consistent with previous observations (7) The role of the SLS motifs in degrading endogenous PML is complicated, because they are not absolutely required for degrading PML.I or its sumoylated forms (although their degradation by mSLS457 is slightly less efficient than by wt), while SLS4 is required for degradation of all forms of PML.II when expressed in isolation (68, 73). Therefore a major component of the PML band remaining in the right-most lane of Fig. 3 is likely to be unsumoylated PML.II. MORC3 was found to be degraded by all mutants analyzed except FXE, indicating the RING finger domain of ICP0, and not the C-terminal region or the SLS motifs, is required for this effect. In this respect the degradation of MORC3 resembles that of PML.I, which is RING finger dependent but SLS motif independent (73). In this latter instance, the degradation of PML.I could be attributed to a direct interaction between ICP0 and PML.I (73). Whether this is the case with MORC3 remains to be determined, although this would not be straightforward to investigate because of the rapidity of MORC3 degradation in the presence of ICP0.

MORC3 is recruited to HSV-1 genomes. Sp100, PML and other PML NB protein components are recruited to HSV-1 genomes entering the nucleus of an infected cell in a process that contributes to the repression of viral gene transcription (54, 55, 62, 74-76). This repression is counteracted by ICP0 mediated degradation of selected PML NB protein components (reviewed in (3)). The assay for the recruitment of PML NB proteins to HSV-1 genomes involves immunofluorescence staining of viral plaques on an infected monolayer of cells with an ICP4 antibody, which acts as a marker for HSV-1 genomes through its efficient association with the viral DNA. Cells at the edges of developing plaques receive a high number of viral genomes, visible as an arc-like pattern just inside the nucleus. This

asymmetric pattern allows unambiguous visualization of recruitment of cellular proteins to sites associated with the viral genome foci. This recruitment is much more readily seen in ICP0 null mutant HSV-1 infections as ICP0 very rapidly counteracts the recruitment process (62). Since MORC3 was reported to colocalize with PML NB proteins, PML and Sp100 (12, 13), and has also been suggested as a DNA binding protein and transcriptional repressor (77), we set out to determine if MORC3 is also recruited to HSV-1 genomes. Due to the rapid degradation of MORC3 following infection we utilized an ICP0-null mutant HSV-1 expressing an EYFP tagged ICP4 (dl0Y4) in order to visualize recruitment more clearly. We infected HFs with dl0Y4 for 24 h at a low MOI and imaged 10 representative cells at the periphery of developing plaques which exhibited ICP4 foci around the nuclear periphery. Immunofluorescence staining for Sp100 was included as a positive control for recruitment and uninfected (mock) cells as a negative control, which confirmed previous reports of MORC3 and Sp100 colocalization (12). As expected, we found close association of Sp100 with EYFP-ICP4 foci around the internal periphery of the nucleus of all newly infected cells, indicative of Sp100 recruitment to HSV-1 genomes entering the nucleus (a typical example is shown in Fig. 4). MORC3 was also in these recruited foci within these cells, demonstrating that MORC3 is indeed recruited to HSV-1 genomes during the initial stages of infection (Fig. 4).

MORC3 influences the recruitment of PML NB components to HSV-1 genomes. The recruitment of the PML NB complex proteins (for example PML, Sp100 and hDaxx) to HSV-1 genomes entering the nucleus of an infected cell occurs independently of each other (55, 74, 76, 78, 79). The precise mechanism responsible for the recruitment of these factors remains unknown, although it has been established that in each of these three cases the presence of a SIM is essential (75). Since MORC3 was recruited to HSV-1 genomes and directly interacts with PML.I, and in one situation is required for Sp100 localizing to PML NBs (12, 13), we investigated whether MORC3 influences the recruitment of these other factors to HSV-1 genomes. In addition, another MORC family protein, MORC2, has been reported to induce phosphorylation of H2AX and the subsequent formation of γH2AX foci and chromatin relaxation (20), which are steps in the pathway to double-strand (ds)-break repair (80). Because it has been established that γH2AX forms regions surrounding replicating HSV-1 genomes in a ds-break repair response (81-83), we therefore included γH2AX in our panel of proteins to investigate whether their recruitment was influenced by MORC3.

To investigate this hypothesis we established HFT and HepaRG cell lines depleted of MORC3 using independent shRNAs, namely shMORC3-1335 and -1339, with the extent of depletion assessed by western blot analysis (Figures 5A). Depletion of MORC3 in HFT- and HA-shMORC3-1339 cells was then confirmed by confocal microscopy, co-staining with PML (Fig. 5B and C, left panels). Since a previous study found depletion of MORC3 from HeLa cells resulted in dispersal of Sp100 (12), we also examined the effect of MORC3 depletion on Sp100 localizing with PML in our cells (Fig. 5B and C, right panels). Surprisingly, in the HFTs examined here, Sp100 remained within PML NBs of uninfected cells when MORC3 was depleted. The difference we observe here may be due to differences in the cell types analyzed, the level of depletion of MORC3 or the antibodies utilized. The great majority of mock infected HFT-shMORC3 cells, of which 95 were imaged, had no detectable MORC3 expression and showed Sp100, PML, hDaxx and γH2AX with the typical nuclear dot formation distributed throughout the nucleus (data not shown).Uninfected HA-shMORC3-1339 cells also displayed Sp100 within PML NBs when MORC3 was more efficiently depleted (Fig. 5C).

Whether MORC3 was required for recruitment of PML, Sp100, hDaxx or γH2AX to sites associated with HSV-1 genomes was assessed by infecting HFT-shMORC3-1339 cells with dl0Y4 (as explained above). Cells were then stained for either PML (FEig. 6A), Sp100, hDaxx, or γH2AX (data not shown) as well as MORC3 to confirm MORC3 depletion in these particular individual cells. Foci of EYFP-ICP4 indicate the localization of HSV-1 genomes and the nucleus was stained with DAPI. HFT-shNeg cells were included as a control in which MORC3 could be co-stained with either Sp100, PML, hDaxx or γH2AX and tested for recruitment to HSV-1 genomes.

Cells that displayed EYFP-ICP4 around the internal nuclear periphery were characterized as newly infected cells with HSV-1 genomes entering the nucleus upon infection (Figure 6A, ICP4+/PML+). We could also identify cells very early following infection due to the rapid recruitment of PML NB proteins to HSV-1 genomes prior to detectable levels of ICP4 expression; such cells have asymmetric PML foci of a type that are never seen in uninfected cells (Figure 6A, ICP4-/PML+). Thus a study that was blinded from the point of view of the observer was performed in which infected, or presumed infected cells surrounding a plaque were identified and divided into the following categories: 1) Those containing foci of both ICP4 and Sp100, PML, γH2AX or hDaxx in close association at the nuclear periphery of a cell (referred to as ICP4+/X+); 2) Those containing foci of Sp100, PML, γH2AX or hDaxx at the nuclear periphery of a cell in the pattern typical of an infected

cell, but prior to detectable expression of ICP4 (referred to as ICP4-/X+); or 3) Those containing ICP4 foci only at the nuclear periphery of a cell, without accompanying foci of the cellular protein in question (referred to as ICP4+/X-) (Fig. 6A). Our analysis showed that in the absence of MORC3 the recruitment of PML was less efficient with 48% of 69 counted cells described as ICP4+/PML- (Fig. 6B). Only 1% of counted cells were assigned as ICP4-/PML+, with the remaining 51% of cells ICP4+/PML+, although visually the abundance of PML foci at the nuclear periphery appeared to be of a lesser degree than the equivalent shNeg control. Of note, some of these shMORC3 cells exhibiting PML recruitment also had low levels of MORC3 remaining and therefore the percentage of cells which are defective for PML recruitment may be higher than described here. Interestingly MORC3 depleted cells that had no PML recruitment to ICP4 foci also no longer contained PML as punctate PML NB structures, suggesting that these structures are less stable in the absence of MORC3 in infected cells, even if ICP0 is not expressed. The corresponding data for the control HFT-shNeg cells indicated 60% of 40 counted cells were ICP4+/PML+ and 35% ICP4-/PML+, indicating that in the presence of MORC3, PML can be recruited very early following infection, prior to detectable ICP4 expression. Only 5% of counted cells were described as ICP4+/PML-. We also investigated the reciprocal effect and found that recruitment of MORC3 was unaffected by depletion of PML (data not shown).

Sp100 recruitment to sites of incoming HSV-1 genomes was also assessed in these MORC3 depleted cells in a similar manner (Fig. 6B and data not shown). We found that in the absence of MORC3, Sp100 is recruited more slowly to viral genomes compared to MORC3 expressing cells. For example, 54% of the 68 counted control HFT-shNeg cells were ICP4+/Sp100+ and 46% ICP4-/Sp100+. Unlike with PML, there were no cells that had ICP4 around the periphery of the nucleus that did not have Sp100 recruited to the same site. However, when MORC3 was depleted only 4% of the 104 counted cells were observed as ICP4-/Sp100+, while 3% of counted cells were ICP4+/Sp100-. The remaining 93% of counted cells were designated ICP4+/Sp100+. Thus the rate of recruitment of Sp100 is decreased in the MORC3 depleted cells. A similar phenotype to Sp100 was seen with γH2AX and hDaxx (Fig. 6B and data not shown), with 47% of the 43 counted HFT-shNeg cells displaying ICP4 and γH2AX foci associated at the nuclear periphery (ICP4+/γH2AX+) and 53% with rapid recruitment of γH2AX to the nuclear periphery prior to ICP4 expression (ICP4-/γH2AX+). In contrast, MORC3 depleted cells displayed 87% of 52 counted cells as ICP4+/γH2AX+, with only the remaining 13% as ICP4-/γH2AX+. Similarly, for hDaxx 66% of 71 counted shNeg cells were described as ICP4+/hDaxx+, 32% as ICP4-/hDaxx+ and the

remaining 1% as ICP4+/hDaxx+. There was evidence of hDaxx recruitment to viral genomes (ICP4+/hDaxx+) in 82% of 71 counted MORC3 depleted cells, while only 3% of counted cells were described as- ICP4-/hDaxx+ and 15% as ICP4+/hDaxx-. Taken together, these results suggest that MORC3 plays a role in the speed or efficiency of recruitment of these PML NB proteins to incoming HSV-1 genomes.

Since PML is required for the formation of PML NBs (84, 85), and was observed as diffuse throughout the nucleus in many of these HFT-shMORC3-1339 dl0Y4 infected cells (Fig 6A and B), it was perhaps surprising to observe some Sp100 remaining as nuclear dots in unrecruited foci. To further assess this observation mock or dl0Y4 infected HFT-shMORC3-1339 cells were dual stained with Sp100 and PML (Fig. 6C). Our analysis confirmed that when PML is nuclear diffuse, Sp100 remains as nuclear dots in both ICP4 associated and unassociated foci. We also observed that in some HFTshMORC3 cells PML staining was apparently less intense than in HFT-shNeg controls, which might be explained by a greater component of diffuse PML distribution.

MORC3 has antiviral activity during HSV-1 and HCMV infection. In previous studies, we have noted a correlation between the recruitment of PML NB components and their role in the restriction of virus gene replication (54, 55, 62, 75, 76) (62, 75, 79, 86), with their functions in this regard counteracted by ICP0 (reviewed in (3)). Since we discovered that MORC3 is recruited to HSV-1 genomes we wanted to determine if MORC3 also has an antiviral role during HSV-1 infection. For these experiments, both HFT and HepaRG (HA) cells that were depleted of MORC3 using shRNAs shMORC3-1335 and -1339 were assessed (Fig. 5A). Viral plaque assays were then performed to compare the plaque formation efficiencies of wt and ICP0-null HSV-1 in these cells (Fig. 7A). Cells expressing a control shRNA (shNeg) were included to normalize plaque numbers. As expected, because of the rapid degradation of MORC3 by ICP0, wt HSV-1 exhibited no change in plaque formation efficiency within both HFT- and HA-shMORC3-1335 and -1339 cells when compared to the shNeg controls (Fig. 7A). However, ICP0-null HSV-1 infection of MORC3 depleted HFT and HA cells resulted in a marked increase in plaque formation efficiency compared to the respective shNeg controls, suggesting that, like several other components of PML NBs, MORC3 has antiviral activity which is counteracted by ICP0. These increases in plaque formation efficiency are at least as marked, even in the most conservative estimation, as the corresponding increases previously seen in cells depleted individually of PML, Sp100 or hDaxx (55, 74, 76).

An increase in plaque formation efficiency would result in increased infectivity of the ICP0-null HSV-1. We therefore confirmed this effect using western blot analysis to detect viral proteins ICP4, UL42 and ICP0 (control for ICP0-null HSV-1). HFT-shMORC3-1339 cells were infected with ICP0-null HSV-1 (dl1403, labeled ΔICP0) at MOI 2 with samples collected over a time course infection. ICP4 and UL42 were expressed at greater levels in the shMORC3 cells compared to the shNeg control, confirming MORC3 depleted cells are more readily infected (Fig. 7B).

HCMV is a beta herpesvirus which is also restricted by the same set of PML NB components as HSV-1, with repression mediated through hDaxx being counteracted by pp71, and through PML being nullified by IE1 (87-93). Therefore we analyzed these MORC3 depleted HFT cells for their ability to restrict HCMV infection using the same controls as listed above (Fig. 7C). The plaque forming efficiency of wt HCMV within HFT-shMORC3 cells was also increased when compared to HFT-shNeg cells, illustrating that MORC3 has antiviral activity towards DNA viruses in addition to HSV-1. The increase in wt HCMV plaque formation in MORC3 depleted cells observed here is reminiscent of that seen in cells depleted of PML or Sp100, indicating that even wt HCMV is sensitive to PML NB component mediated restriction (as described in the studies cited above).

DISCUSSION

Here we report an antiviral function for the nuclear matrix protein, MORC3. Our previous study identified sumoylated MORC3 as a degradation target of the HSV-1 E3 ubiquitin ligase protein, ICP0 (9), which led us to further investigate the function of MORC3 during HSV-1 infection. Until now the role of MORC3 during virus infections was relatively unknown, although one other report suggested that MORC3 was required for efficient Influenza A virus (IAV) infection (50). MORC3 is a sumoylated nuclear matrix protein with RNA and DNA binding activities (13, 17), which associates with PML NBs. This association is through a SUMO-SIM interaction with PML.I, which requires a functional ATPase domain within MORC3 (12, 13). In our analysis of HFT cells, we found that MORC3 was detectable in only a subset of PML NBs, whereas others reported that in HeLa and Saos-2 cells MORC3 was colocalized to majority of PML nuclear foci. This difference in detail may be due to cell type or efficiency of antibody detection, and indeed Ver *et al* found no significant colocalization of MORC3 with PML in A549 cells (50). One reported role of MORC3 in PML NBs is to recruit Sp100 and p53 into these complexes (12), although in the HF-derived cells used here

the former function was not evident. The discrepancy may be due to differences in cell types examined or the efficiency of MORC3 depletion.

Upon infection with HSV-1 there is activation of an intrinsic immune response including recruitment of protein components of the PML NB complex, including PML, Sp100 and hDaxx, independently to sites associated with HSV-1 genomes entering the infected cell nucleus. In the absence of ICP0, this recruitment contributes to cell-mediated repression of viral gene replication (54, 55, 62, 74, 76, 94). The DNA repair protein γH2AX also accumulates in regions surrounding the viral genomes (82, 83). The repression mediated through the recruitment of PML NB components is counteracted by the expression of ICP0 which preferentially degrades sumoylated forms of these proteins, and causes dispersion of others (7, 8, 64-67). The association of MORC3 with PML NBs in uninfected cells led us to investigate the recruitment of MORC3 to HSV-1 genomes during the initial stages of infection, which led to the finding that MORC3 becomes associated with foci of ICP4 in a similar manner to the well characterized behavior of PML NB components. This provoked some intriguing questions as to the role of MORC3 during an intrinsic immune response to HSV-1 infection. We found that PML recruitment was noticeably affected in MORC3 depleted cells, and that Sp100, γH2AX and hDaxx were also recruited less efficiently, although this defect was not as marked as that of PML. In control cells, there appears to be a temporal transfer of PML protein from PML NBs to ICP4-associated foci, such that foci of both types can frequently be observed in the infected cells. However, in a large number of MORC3 depleted ICP0-null infected cells the PML signal becomes disperse with neither PML NB-like nor recruited foci. This observation is very intriguing since we still see Sp100 in nuclear foci despite the fact that PML is required for the formation of PML NB complexes (84, 85). Since these PML NB complexes are dynamic, the lack of detectable punctate nuclear PML foci in these cells may be due to a change in the equilibrium of PML shuttling in and out of these structures in a manner that is in some way influenced by MORC3.

Our HSV-1 viral plaque assays in MORC3 depleted cells indicated that MORC3 has antiviral functions that are counteracted in the presence of ICP0, thus providing the first report of evidence for an antiviral role for MORC3. To enhance the repertoire of viruses investigated for the role of MORC3 we also assessed the replication efficiency of the beta-herpesvirus, human cytomegalovirus (HCMV). Like HSV-1, HCMV also counteracts the PML NB mediated repression of its viral gene transcription (87-93, 95). Infection of our MORC3 depleted cells with wt HCMV resulted in an increase in plaque formation efficiency when compared to the control cells. Therefore MORC3 has antiviral activity towards DNA

viruses in addition to HSV-1. It would be of interest to examine other herpesviruses in the future to determine if this response is general to all herpesviruses.

In summary, we report that MORC3 has an antiviral role during HSV-1 and HCMV infection. The antiviral effect of MORC3 during HSV-1 infection was counteracted by the viral ubiquitin ligase protein, ICP0, and we identified that depletion of MORC3 reduces the efficiency of recruitment of PML NB component proteins to HSV-1 genomes. Because the recruitment of these PML NB proteins plays an important role during the intrinsic immune response to HSV-1, this role of MORC3 may underlie why restriction of ICP0-null HSV-1 is reduced in its absence. It is notable that our interest in MORC3 came through a general screen of changes in the SUMO2 proteome during HSV-1 infection which eventually and independently led to connections with PML NB mediated restriction, thus underlining the biological relevance of virus-PML NB interactions. This study has provided further insight to the understanding of the intrinsic immune response to HSV-1 and opens a new avenue of research into MORC3 beyond herpesviruses.

ACKNOWLEDGMENTS

We are very grateful for the gifts of the indicated reagents from the following people: antibodies from Roel van Driel (PML 5E10) and Hans Will (SpGH and Sp26); HSV-1 *in*1863 and *dl*1403/CMV*lac*Z from Chris Preston; plasmid pCMV.DR.8.91 from Didier Trono.

FUNDING INFORMATION

Medical Research Council (MRC) provided funding to Roger D. Everett under grant number MC_UU_12014/4. The funder had no role in study design, data collection and interpretation, or the decision to submit the work for publication.

REFERENCES

FIGURE LEGENDS

Fig. 1: MORC3 associates with Sp100 in PML NBs and ICP0 early during wt HSV-1 infection and is subsequently degraded. HFs were either mock infected or infected with wt HSV-1 (MOI 2), fixed and permeabilized at 1 or 2 h post infection. Cells were analyzed for association of MORC3 (Novus Biologicals) (red) with Sp100 (top row, showing concentrations of MORC3 associated with Sp100 in a variable manner; see also Fig. 4), and

with ICP0 (11060) (green) in infected cells using confocal microscopy. The blue signal in the merged channel is DAPI. The arrow indicates a cell with ICP0 in association with MORC3. The MORC3 signal diminishes as infection progresses.

Fig. 2: MORC3 is degraded in an ICP0 dependent manner. HFT cells were infected at MOI 20 with an ICP0 null HSV-1 (ΔICP0) and lyzed at 3, 6, and 9 h p.i. for western blot analysis. Analysis of PML abundance and wt HSV-1 infected (MOI 2) lysates prepared in parallel were included as positive controls for degradation. Membranes were probed with anti-MORC3 (Novus Biologicals) and anti-PML (5E10) antibodies, with anti-tubulin (Sigma-Aldrich) used as a loading control. Viral proteins ICP4 and UL42 were included to show equivalent infection between wt and ΔICP0 HSV-1.

Fig. 3: RING finger domain of ICP0 is required for MORC3 degradation. (A) Schematic diagram of ICP0 displaying internal domains and SIM-like sequences (SLS) as well as regions of mutations/deletions of the RING finger (FXE) and C-terminal (E52X) domains. (B) HA-TetR (control) and HA-cICP0, -cICP0 FXE (Δ149-160), -cICP0 E52X (Δ594-775), -cICP0 mSLS4, and -cICP0 mSLS457 cells with the ability to express wt and mutant forms of ICP0 were treated with doxycycline (Dox) (+) or left untreated (-) then analyzed by western blot. Membranes were probed with anti-MORC3 (Novus Biologicals), -ICP0 (11060), and -PML (5E10) antibodies, with anti-tubulin (Sigma-Aldrich) included as a loading control.

Fig. 4: MORC3 is recruited to HSV-1 genomes during the initial stage of infection. HFs were infected at low MOI with dl0Y4 for 24 h, fixed, permeablized and probed with anti-MORC3 antibody (Novus Biologicals) (purple). Anti-Sp100 (Sp26) (red) was included as a positive control for recruitment to viral genomes, with nuclei stained with DAPI (blue). Recruitment to ICP4 was visualized by confocal microscopy (right-hand column), compared to a typical uninfected cell (left-hand column).

Fig. 5: Characterization of MORC3 depleted cells. (A) Generation of MORC3 depleted HFT (HFT-shMORC3-1335 and -1339 cells) and HepaRG cells (HA-shMORC3-1335, -1337 and -1339 cells) using shRNAs expressed from lentiviral vectors. Total protein lysates were analyzed by western blot to determine level of MORC3 depletion with HFT-shNeg and HepaRG cells included as controls. Tubulin was included as a loading control. Characterization of MORC3 depleted HFT cells (B) and HepaRG cells (C). Mock HFT- and

HA-shMORC3-1339 and control cells were immuno-stained for PML (red) and MORC3 (green) (left panels), and Sp100 (green) and PML (red) (right panels) to confirm MORC3 depletion and assess effects on PML NBs. DAPI staining of the nuclei is shown in blue in the merged panels.

Fig. 6: Recruitment of PML NB proteins to viral DNA is diminished in the absence of MORC3. (A) HFT-shMORC3-1339 and -shNeg cells were infected with dl0Y4 (MOI 2) for 24 h. Cells were immuno-stained using PML (5E10) (red), MORC3 (Novus biologicals) (blue) and nuclei stained with DAPI (far right panels) and visualized by confocal microscopy. Infected, or presumed infected cells surrounding a plaque were counted and divided into three categories which are represented here. *Category 1*: ICP4+/PML+ (foci of ICP4 and PML in close association at the nuclear periphery of a cell), C*ategory 2*: ICP4-/PML+ (foci of PML at the nuclear periphery of a cell in the pattern typical of an infected cell, but prior to detectable expression of ICP4), or *Category 3*: ICP4+/PML- (ICP4 foci only at the nuclear periphery of a cell). (B) Percentages of cells within each category are presented in bar graphs. Sp100, hDaxx and γH2AX were also assessed as described for PML with results represented as bar graphs. (C) HFT-shMORC3-1339 and -shNeg cells were infected with dl0Y4 (MOI 2) for 24 h. Cells were immuno-stained using Sp100 (Sp26) (Red), PML (5E10) (blue) and nuclei were stained with DAPI (far right panels), while ICP4 was detected by the EYFP signal.

Fig. 7: MORC3 has antiviral activity during ICP0-null mutant HSV-1 and wt HCMV. (A) Data from several independent viral plaque assays of both wt and ΔICP0 HSV-1 infected HFT- and HA- shMORC3-1335 and -1339 cells were averaged and normalized to the respective shNeg cell controls and plotted ± standard deviation. (B) Western blot analysis comparing infection efficiency of ΔICP0 HSV-1 within HFT-shMORC3-1339 and HFT-shNeg cells over a time course infection. Cells were infected at MOI 2 with ΔICP0 HSV-1 and lyzed at 2, 4, or 6 h p.i., and probed for ICP4, ICP0, UL42 and actin loading control. (C) HCMV viral plaque forming efficiencies using HFT-shMORC3-1335 and -1339 cells normalized to HFT-shNeg cells and plotted ± standard deviation.

REFERENCES

1. **Knipe D, Howley P, Griffin D, Lamb R, Martin M, Roizman B, Strauss S.** 2006 Fields Virology. Philadelphia: Lippincott Williams and Wilkins.

2. **Weller S.** 2011. Alphaherpesviruses. Norfolk, U.K.: Caister Academic Press.
3. **Boutell C, Everett RD.** 2013. Regulation of alphaherpesvirus infections by the ICP0 family of proteins. J Gen Virol **94:**465-481.
4. **Geoffroy MC, Chelbi-Alix MK.** 2011. Role of promyelocytic leukemia protein in host antiviral defense. J Interferon Cytokine Res **31:**145-158.
5. **Everett RD, Boutell C, Hale BG.** 2013. Interplay between viruses and host sumoylation pathways. Nat Rev Microbiol **11:**400-411.
6. **Tavalai N, Stamminger T.** 2008. New insights into the role of the subnuclear structure ND10 for viral infection. Biochim Biophys Acta **1783:**2207-2221.
7. **Boutell C, Cuchet-Lourenco D, Vanni E, Orr A, Glass M, McFarlane S, Everett RD.** 2011. A viral ubiquitin ligase has substrate preferential SUMO targeted ubiquitin ligase activity that counteracts intrinsic antiviral defence. PLoS Pathog **7:**e1002245.
8. **Everett RD, Freemont P, Saitoh H, Dasso M, Orr A, Kathoria M, Parkinson J.** 1998. The disruption of ND10 during herpes simplex virus infection correlates with the Vmw110- and proteasome-dependent loss of several PML isoforms. J Virol **72:**6581-6591.
9. **Sloan E, Tatham MH, Groslambert M, Glass M, Orr A, Hay RT, Everett RD.** 2015. Analysis of the SUMO2 Proteome during HSV-1 Infection. PLoS Pathog **11:**e1005059.
10. **Iyer LM, Abhiman S, Aravind L.** 2008. MutL homologs in restriction-modification systems and the origin of eukaryotic MORC ATPases. Biol Direct **3:**8.
11. **Iyer LM, Anantharaman V, Wolf MY, Aravind L.** 2008. Comparative genomics of transcription factors and chromatin proteins in parasitic protists and other eukaryotes. Int J Parasitol **38:**1-31.
12. **Takahashi K, Yoshida N, Murakami N, Kawata K, Ishizaki H, Tanaka-Okamoto M, Miyoshi J, Zinn AR, Shime H, Inoue N.** 2007. Dynamic regulation of p53 subnuclear localization and senescence by MORC3. Mol Biol Cell **18:**1701-1709.
13. **Mimura Y, Takahashi K, Kawata K, Akazawa T, Inoue N.** 2010. Two-step colocalization of MORC3 with PML nuclear bodies. J Cell Sci **123:**2014-2024.
14. **Dutta R, Inouye M.** 2000. GHKL, an emergent ATPase/kinase superfamily. Trends Biochem Sci **25:**24-28.
15. **Perry J, Zhao Y.** 2003. The CW domain, a structural module shared amongst vertebrates, vertebrate-infecting parasites and higher plants. Trends Biochem Sci **28:**576-580.
16. **Inoue N, Hess KD, Moreadith RW, Richardson LL, Handel MA, Watson ML, Zinn AR.** 1999. New gene family defined by MORC, a nuclear protein required for mouse spermatogenesis. Hum Mol Genet **8:**1201-1207.
17. **Kimura Y, Sakai F, Nakano O, Kisaki O, Sugimoto H, Sawamura T, Sadano H, Osumi T.** 2002. The newly identified human nuclear protein NXP-2 possesses three distinct domains, the nuclear matrix-binding, RNA-binding, and coiled-coil domains. J Biol Chem **277:**20611-20617.
18. **Moissiard G, Cokus SJ, Cary J, Feng S, Billi AC, Stroud H, Husmann D, Zhan Y, Lajoie BR, McCord RP, Hale CJ, Feng W, Michaels SD, Frand AR, Pellegrini M, Dekker J, Kim JK, Jacobsen SE.** 2012. MORC family ATPases required for heterochromatin condensation and gene silencing. Science **336:**1448-1451.
19. **Lorkovic ZJ, Naumann U, Matzke AJ, Matzke M.** 2012. Involvement of a GHKL ATPase in RNA-directed DNA methylation in Arabidopsis thaliana. Curr Biol **22:**933-938.
20. **Li DQ, Nair SS, Ohshiro K, Kumar A, Nair VS, Pakala SB, Reddy SD, Gajula RP, Eswaran J, Aravind L, Kumar R.** 2012. MORC2 signaling integrates

phosphorylation-dependent, ATPase-coupled chromatin remodeling during the DNA damage response. Cell Rep **2:**1657-1669.

21. **He F, Umehara T, Saito K, Harada T, Watanabe S, Yabuki T, Kigawa T, Takahashi M, Kuwasako K, Tsuda K, Matsuda T, Aoki M, Seki E, Kobayashi N, Guntert P, Yokoyama S, Muto Y.** 2010. Structural insight into the zinc finger CW domain as a histone modification reader. Structure **18:**1127-1139.
22. **Hoppmann V, Thorstensen T, Kristiansen PE, Veiseth SV, Rahman MA, Finne K, Aalen RB, Aasland R.** 2011. The CW domain, a new histone recognition module in chromatin proteins. EMBO J **30:**1939-1952.
23. **Li X, Foley EA, Molloy KR, Li Y, Chait BT, Kapoor TM.** 2012. Quantitative chemical proteomics approach to identify post-translational modification-mediated protein-protein interactions. J Am Chem Soc **134:**1982-1985.
24. **Hurme R, Berndt KD, Namork E, Rhen M.** 1996. DNA binding exerted by a bacterial gene regulator with an extensive coiled-coil domain. J Biol Chem **271:**12626-12631.
25. **Nikolay R, Wiederkehr T, Rist W, Kramer G, Mayer MP, Bukau B.** 2004. Dimerization of the human E3 ligase CHIP via a coiled-coil domain is essential for its activity. J Biol Chem **279:**2673-2678.
26. **Parachoniak CA, Park M.** 2009. Distinct recruitment of Eps15 via Its coiled-coil domain is required for efficient down-regulation of the met receptor tyrosine kinase. J Biol Chem **284:**8382-8394.
27. **Rairdan GJ, Collier SM, Sacco MA, Baldwin TT, Boettrich T, Moffett P.** 2008. The coiled-coil and nucleotide binding domains of the Potato Rx disease resistance protein function in pathogen recognition and signaling. Plant Cell **20:**739-751.
28. **He Y, Wertheim JA, Xu L, Miller JP, Karnell FG, Choi JK, Ren R, Pear WS.** 2002. The coiled-coil domain and Tyr177 of bcr are required to induce a murine chronic myelogenous leukemia-like disease by bcr/abl. Blood **99:**2957-2968.
29. **Cheng HY, Schiavone AP, Smithgall TE.** 2001. A point mutation in the N-terminal coiled-coil domain releases c-Fes tyrosine kinase activity and survival signaling in myeloid leukemia cells. Mol Cell Biol **21:**6170-6180.
30. **Zhang X, Subrahmanyam R, Wong R, Gross AW, Ren R.** 2001. The NH(2)-terminal coiled-coil domain and tyrosine 177 play important roles in induction of a myeloproliferative disease in mice by Bcr-Abl. Mol Cell Biol **21:**840-853.
31. **Lupas AN, Gruber M.** 2005. The structure of alpha-helical coiled coils. Adv Protein Chem **70:**37-78.
32. **Li X, He L, Che KH, Funderburk SF, Pan L, Pan N, Zhang M, Yue Z, Zhao Y.** 2012. Imperfect interface of Beclin1 coiled-coil domain regulates homodimer and heterodimer formation with Atg14L and UVRAG. Nat Commun **3:**662.
33. **Burkhard P, Stetefeld J, Strelkov SV.** 2001. Coiled coils: a highly versatile protein folding motif. Trends Cell Biol **11:**82-88.
34. **Cheng P, Yang Y, Heintzen C, Liu Y.** 2001. Coiled-coil domain-mediated FRQ-FRQ interaction is essential for its circadian clock function in Neurospora. EMBO J **20:**101-108.
35. **Peng H, Begg GE, Schultz DC, Friedman JR, Jensen DE, Speicher DW, Rauscher FJ, 3rd.** 2000. Reconstitution of the KRAB-KAP-1 repressor complex: a model system for defining the molecular anatomy of RING-B box-coiled-coil domain-mediated protein-protein interactions. J Mol Biol **295:**1139-1162.
36. **Buisson R, Masson JY.** 2012. PALB2 self-interaction controls homologous recombination. Nucleic Acids Res **40:**10312-10323.

37. **Hohl M, Kwon Y, Galvan SM, Xue X, Tous C, Aguilera A, Sung P, Petrini JH.** 2011. The Rad50 coiled-coil domain is indispensable for Mre11 complex functions. Nat Struct Mol Biol **18:**1124-1131.
38. **Itakura E, Sawada I, Matsuura A.** 2005. Dimerization of the ATRIP protein through the coiled-coil motif and its implication to the maintenance of stalled replication forks. Mol Biol Cell **16:**5551-5562.
39. **Ball HL, Cortez D.** 2005. ATRIP oligomerization is required for ATR-dependent checkpoint signaling. J Biol Chem **280:**31390-31396.
40. **Ma J, Zhang T, Novotny-Diermayr V, Tan AL, Cao X.** 2003. A novel sequence in the coiled-coil domain of Stat3 essential for its nuclear translocation. J Biol Chem **278:**29252-29260.
41. **Raiborg C, Bremnes B, Mehlum A, Gillooly DJ, D'Arrigo A, Stang E, Stenmark H.** 2001. FYVE and coiled-coil domains determine the specific localisation of Hrs to early endosomes. J Cell Sci **114:**2255-2263.
42. **Begitt A, Meyer T, van Rossum M, Vinkemeier U.** 2000. Nucleocytoplasmic translocation of Stat1 is regulated by a leucine-rich export signal in the coiled-coil domain. Proc Natl Acad Sci U S A **97:**10418-10423.
43. **Blazek D, Barboric M, Kohoutek J, Oven I, Peterlin BM.** 2005. Oligomerization of HEXIM1 via 7SK snRNA and coiled-coil region directs the inhibition of P-TEFb. Nucleic Acids Res **33:**7000-7010.
44. **Li DQ, Nair SS, Kumar R.** 2013. The MORC family: new epigenetic regulators of transcription and DNA damage response. Epigenetics **8:**685-693.
45. **Condomines M, Hose D, Raynaud P, Hundemer M, De Vos J, Baudard M, Moehler T, Pantesco V, Moos M, Schved JF, Rossi JF, Reme T, Goldschmidt H, Klein B.** 2007. Cancer/testis genes in multiple myeloma: expression patterns and prognosis value determined by microarray analysis. J Immunol **178:**3307-3315.
46. **Shah SP, Morin RD, Khattra J, Prentice L, Pugh T, Burleigh A, Delaney A, Gelmon K, Guliany R, Senz J, Steidl C, Holt RA, Jones S, Sun M, Leung G, Moore R, Severson T, Taylor GA, Teschendorff AE, Tse K, Turashvili G, Varhol R, Warren RL, Watson P, Zhao Y, Caldas C, Huntsman D, Hirst M, Marra MA, Aparicio S.** 2009. Mutational evolution in a lobular breast tumour profiled at single nucleotide resolution. Nature **461:**809-813.
47. **Tripathi A, King C, de la Morenas A, Perry VK, Burke B, Antoine GA, Hirsch EF, Kavanah M, Mendez J, Stone M, Gerry NP, Lenburg ME, Rosenberg CL.** 2008. Gene expression abnormalities in histologically normal breast epithelium of breast cancer patients. Int J Cancer **122:**1557-1566.
48. **Chen LH, Kuo WH, Tsai MH, Chen PC, Hsiao CK, Chuang EY, Chang LY, Hsieh FJ, Lai LC, Chang KJ.** 2011. Identification of prognostic genes for recurrent risk prediction in triple negative breast cancer patients in Taiwan. PLoS One **6:**e28222.
49. **Liggins AP, Cooper CD, Lawrie CH, Brown PJ, Collins GP, Hatton CS, Pulford K, Banham AH.** 2007. MORC4, a novel member of the MORC family, is highly expressed in a subset of diffuse large B-cell lymphomas. Br J Haematol **138:**479-486.
50. **Ver LS, Marcos-Villar L, Landeras-Bueno S, Nieto A, Ortin J.** 2015. The Cellular Factor NXP2/MORC3 Is a Positive Regulator of Influenza Virus Multiplication. J Virol **89:**10023-10030.
51. **Stow ND, Stow EC.** 1986. Isolation and characterization of a herpes simplex virus type 1 mutant containing a deletion within the gene encoding the immediate early polypeptide Vmw110. J Gen Virol **67 (Pt 12):**2571-2585.

52. **Cuchet-Lourenco D, Anderson G, Sloan E, Orr A, Everett RD.** 2013. The viral ubiquitin ligase ICP0 is neither sufficient nor necessary for degradation of the cellular DNA sensor IFI16 during herpes simplex virus 1 infection. J Virol **87:**13422-13432.
53. **Gripon P, Rumin S, Urban S, Le Seyec J, Glaise D, Cannie I, Guyomard C, Lucas J, Trepo C, Guguen-Guillouzo C.** 2002. Infection of a human hepatoma cell line by hepatitis B virus. Proc Natl Acad Sci U S A **99:**15655-15660.
54. **Everett RD, Parsy ML, Orr A.** 2009. Analysis of the functions of herpes simplex virus type 1 regulatory protein ICP0 that are critical for lytic infection and derepression of quiescent viral genomes. J Virol **83:**4963-4977.
55. **Everett RD, Rechter S, Papior P, Tavalai N, Stamminger T, Orr A.** 2006. PML contributes to a cellular mechanism of repression of herpes simplex virus type 1 infection that is inactivated by ICP0. J Virol **80:**7995-8005.
56. **Jamieson DR, Robinson LH, Daksis JI, Nicholl MJ, Preston CM.** 1995. Quiescent viral genomes in human fibroblasts after infection with herpes simplex virus type 1 Vmw65 mutants. J Gen Virol **76 (Pt 6):**1417-1431.
57. **Stuurman N, de Graaf A, Floore A, Josso A, Humbel B, de Jong L, van Driel R.** 1992. A monoclonal antibody recognizing nuclear matrix-associated nuclear bodies. J Cell Sci **101 (Pt 4):**773-784.
58. **Everett RD, Cross A, Orr A.** 1993. A truncated form of herpes simplex virus type 1 immediate-early protein Vmw110 is expressed in a cell type dependent manner. Virology **197:**751-756.
59. **Showalter SD, Zweig M, Hampar B.** 1981. Monoclonal antibodies to herpes simplex virus type 1 proteins, including the immediate-early protein ICP 4. Infect Immun **34:**684-692.
60. **Schenk P, Ludwig H.** 1988. The 65 K DNA binding protein appears early in HSV-1 replication. Arch Virol **102:**119-123.
61. **Guldner HH, Szostecki C, Schroder P, Matschl U, Jensen K, Luders C, Will H, Sternsdorf T.** 1999. Splice variants of the nuclear dot-associated Sp100 protein contain homologies to HMG-1 and a human nuclear phosphoprotein-box motif. J Cell Sci **112 (Pt 5):**733-747.
62. **Everett RD, Murray J.** 2005. ND10 components relocate to sites associated with herpes simplex virus type 1 nucleoprotein complexes during virus infection. J Virol **79:**5078-5089.
63. **Grotzinger T, Sternsdorf T, Jensen K, Will H.** 1996. Interferon-modulated expression of genes encoding the nuclear-dot-associated proteins Sp100 and promyelocytic leukemia protein (PML). Eur J Biochem **238:**554-560.
64. **Maul GG, Guldner HH, Spivack JG.** 1993. Modification of discrete nuclear domains induced by herpes simplex virus type 1 immediate early gene 1 product (ICP0). J Gen Virol **74 (Pt 12):**2679-2690.
65. **Muller S, Dejean A.** 1999. Viral immediate-early proteins abrogate the modification by SUMO-1 of PML and Sp100 proteins, correlating with nuclear body disruption. J Virol **73:**5137-5143.
66. **Chelbi-Alix MK, de The H.** 1999. Herpes virus induced proteasome-dependent degradation of the nuclear bodies-associated PML and Sp100 proteins. Oncogene **18:**935-941.
67. **Parkinson J, Everett RD.** 2000. Alphaherpesvirus proteins related to herpes simplex virus type 1 ICP0 affect cellular structures and proteins. J Virol **74:**10006-10017.
68. **Everett RD, Boutell C, Pheasant K, Cuchet-Lourenco D, Orr A.** 2014. Sequences related to SUMO interaction motifs in herpes simplex virus 1 protein ICP0 act cooperatively to stimulate virus infection. J Virol **88:**2763-2774.

69. **Fukuyo Y, Horikoshi N, Ishov AM, Silverstein SJ, Nakajima T.** 2011. The herpes simplex virus immediate-early ubiquitin ligase ICP0 induces degradation of the ICP0 repressor protein E2FBP1. J Virol **85:**3356-3366.
70. **Everett RD, Meredith M, Orr A, Cross A, Kathoria M, Parkinson J.** 1997. A novel ubiquitin-specific protease is dynamically associated with the PML nuclear domain and binds to a herpesvirus regulatory protein. EMBO J **16:**1519-1530.
71. **Gu H, Roizman B.** 2007. Herpes simplex virus-infected cell protein 0 blocks the silencing of viral DNA by dissociating histone deacetylases from the CoREST-REST complex. Proc Natl Acad Sci U S A **104:**17134-17139.
72. **Hagglund R, Roizman B.** 2002. Characterization of the novel E3 ubiquitin ligase encoded in exon 3 of herpes simplex virus-1-infected cell protein 0. Proc Natl Acad Sci U S A **99:**7889-7894.
73. **Cuchet-Lourenco D, Vanni E, Glass M, Orr A, Everett RD.** 2012. Herpes simplex virus 1 ubiquitin ligase ICP0 interacts with PML isoform I and induces its SUMO-independent degradation. J Virol **86:**11209-11222.
74. **Lukashchuk V, Everett RD.** 2010. Regulation of ICP0-null mutant herpes simplex virus type 1 infection by ND10 components ATRX and hDaxx. J Virol **84:**4026-4040.
75. **Cuchet-Lourenco D, Boutell C, Lukashchuk V, Grant K, Sykes A, Murray J, Orr A, Everett RD.** 2011. SUMO pathway dependent recruitment of cellular repressors to herpes simplex virus type 1 genomes. PLoS Pathog **7:**e1002123.
76. **Everett RD, Parada C, Gripon P, Sirma H, Orr A.** 2008. Replication of ICP0-null mutant herpes simplex virus type 1 is restricted by both PML and Sp100. J Virol **82:**2661-2672.
77. **Rosendorff A, Sakakibara S, Lu S, Kieff E, Xuan Y, DiBacco A, Shi Y, Shi Y, Gill G.** 2006. NXP-2 association with SUMO-2 depends on lysines required for transcriptional repression. Proc Natl Acad Sci U S A **103:**5308-5313.
78. **Everett RD, Murray J, Orr A, Preston CM.** 2007. Herpes simplex virus type 1 genomes are associated with ND10 nuclear substructures in quiescently infected human fibroblasts. J Virol **81:**10991-11004.
79. **Everett RD, Chelbi-Alix MK.** 2007. PML and PML nuclear bodies: implications in antiviral defence. Biochimie **89:**819-830.
80. **Rogakou EP, Pilch DR, Orr AH, Ivanova VS, Bonner WM.** 1998. DNA double-stranded breaks induce histone H2AX phosphorylation on serine 139. J Biol Chem **273:**5858-5868.
81. **Wilkinson DE, Weller SK.** 2006. Herpes simplex virus type I disrupts the ATR-dependent DNA-damage response during lytic infection. J Cell Sci **119:**2695-2703.
82. **Weller SK.** 2010. Herpes simplex virus reorganizes the cellular DNA repair and protein quality control machinery. PLoS Pathog **6:**e1001105.
83. **Lilley CE, Chaurushiya MS, Boutell C, Everett RD, Weitzman MD.** 2011. The intrinsic antiviral defense to incoming HSV-1 genomes includes specific DNA repair proteins and is counteracted by the viral protein ICP0. PLoS Pathog **7:**e1002084.
84. **Ishov AM, Sotnikov AG, Negorev D, Vladimirova OV, Neff N, Kamitani T, Yeh ET, Strauss JF, 3rd, Maul GG.** 1999. PML is critical for ND10 formation and recruits the PML-interacting protein daxx to this nuclear structure when modified by SUMO-1. J Cell Biol **147:**221-234.
85. **Zhong S, Muller S, Ronchetti S, Freemont PS, Dejean A, Pandolfi PP.** 2000. Role of SUMO-1-modified PML in nuclear body formation. Blood **95:**2748-2752.
86. **Saffert RT, Kalejta RF.** 2008. Promyelocytic leukemia-nuclear body proteins: herpesvirus enemies, accomplices, or both? Future Virol **3:**265-277.

87. **Preston CM, Nicholl MJ.** 2006. Role of the cellular protein hDaxx in human cytomegalovirus immediate-early gene expression. J Gen Virol **87:**1113-1121.
88. **Saffert RT, Kalejta RF.** 2006. Inactivating a cellular intrinsic immune defense mediated by Daxx is the mechanism through which the human cytomegalovirus pp71 protein stimulates viral immediate-early gene expression. J Virol **80:**3863-3871.
89. **Woodhall DL, Groves IJ, Reeves MB, Wilkinson G, Sinclair JH.** 2006. Human Daxx-mediated repression of human cytomegalovirus gene expression correlates with a repressive chromatin structure around the major immediate early promoter. J Biol Chem **281:**37652-37660.
90. **Kim YE, Lee JH, Kim ET, Shin HJ, Gu SY, Seol HS, Ling PD, Lee CH, Ahn JH.** 2011. Human cytomegalovirus infection causes degradation of Sp100 proteins that suppress viral gene expression. J Virol **85:**11928-11937.
91. **Tavalai N, Papior P, Rechter S, Leis M, Stamminger T.** 2006. Evidence for a role of the cellular ND10 protein PML in mediating intrinsic immunity against human cytomegalovirus infections. J Virol **80:**8006-8018.
92. **Tavalai N, Papior P, Rechter S, Stamminger T.** 2008. Nuclear domain 10 components promyelocytic leukemia protein and hDaxx independently contribute to an intrinsic antiviral defense against human cytomegalovirus infection. J Virol **82:**126-137.
93. **Tavalai N, Adler M, Scherer M, Riedl Y, Stamminger T.** 2011. Evidence for a dual antiviral role of the major nuclear domain 10 component Sp100 during the immediate-early and late phases of the human cytomegalovirus replication cycle. J Virol **85:**9447-9458.
94. **Glass M, Everett RD.** 2013. Components of promyelocytic leukemia nuclear bodies (ND10) act cooperatively to repress herpesvirus infection. J Virol **87:**2174-2185.
95. **Ahn JH, Hayward GS.** 2000. Disruption of PML-associated nuclear bodies by IE1 correlates with efficient early stages of viral gene expression and DNA replication in human cytomegalovirus infection. Virology **274:**39-55.

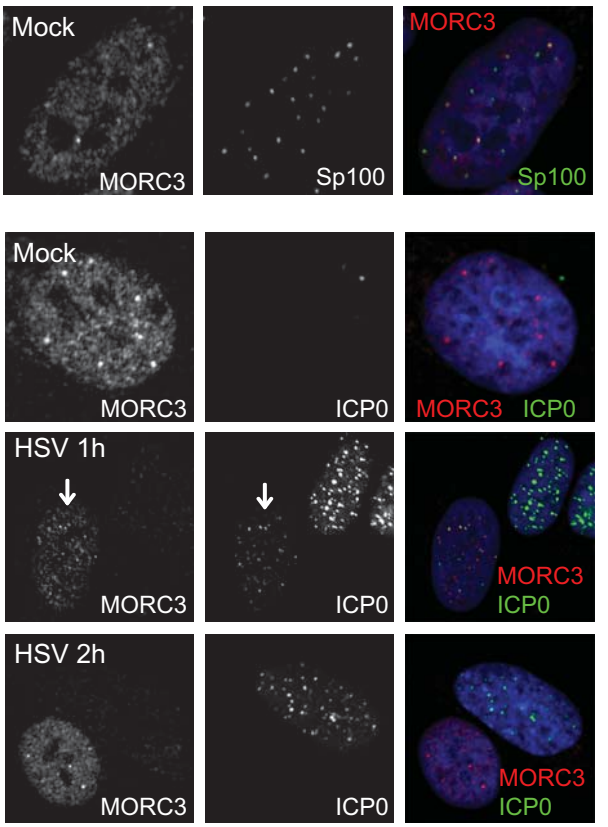
Mock
MORC3
Sp100
MORC3
Sp100
Mock
MORC3
ICP0
MORC3
ICP0
HSV 1h
MORC3
ICP0
MORC3
ICP0
HSV 2h
MORC3
ICP0
MORC3
ICP0

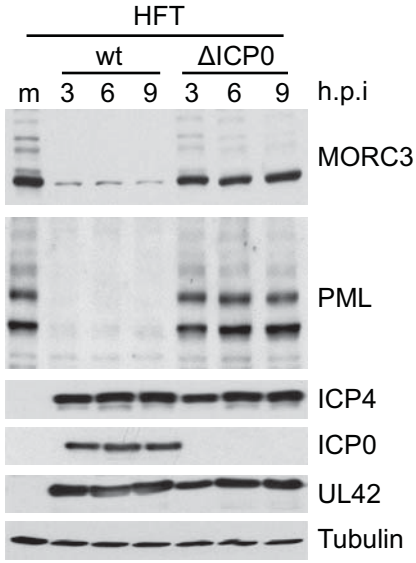
HFT
wt
ΔICP0
m
3
6
9
3
6
9
h.p.i
MORC3
PML
ICP4
ICP0
UL42
Tubulin

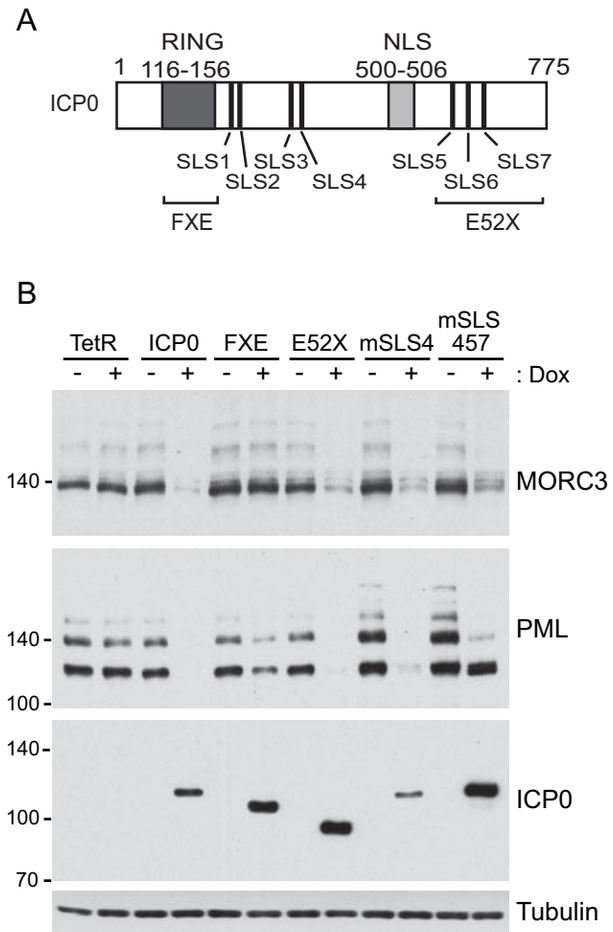
A
RING
116-156
NLS
500-506
1
775
ICP0
SLS1
SLS2
SLS3
SLS4
SLS5
SLS6
SLS7
FXE
E52X
B
TetR
ICP0
FXE
E52X
mSLS4
mSLS
457
- + - + - + - + - + - +
: Dox
140
MORC3
140
100
PML
140
100
70
ICP0
Tubulin

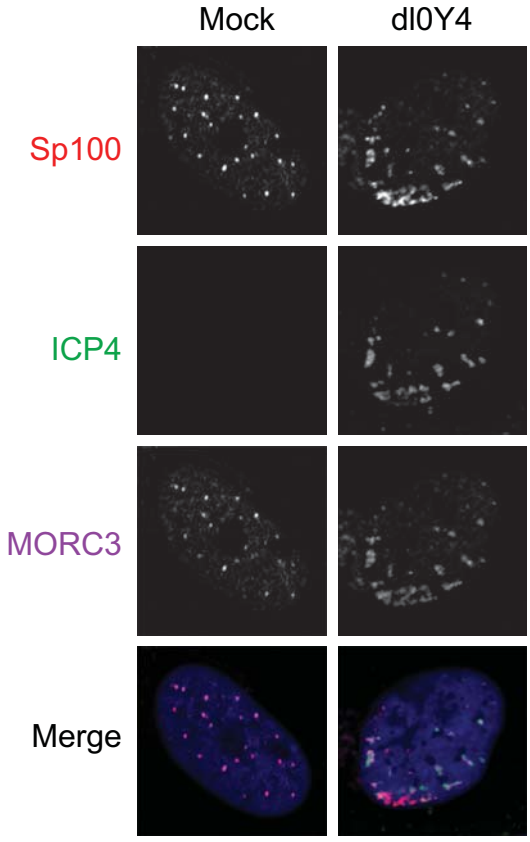
Mock
dl0Y4
Sp100
ICP4
MORC3
Merge

A

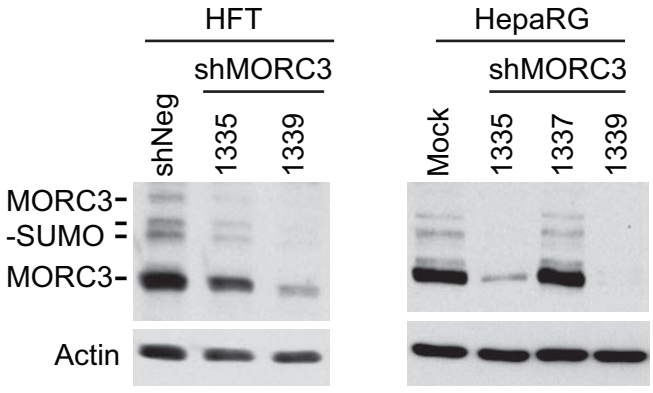
HFT
shMORC3
shNeg
1335
1339
HepaRG
shMORC3
Mock
1335
1337
1339
MORC3
-SUMO
MORC3
Actin

B

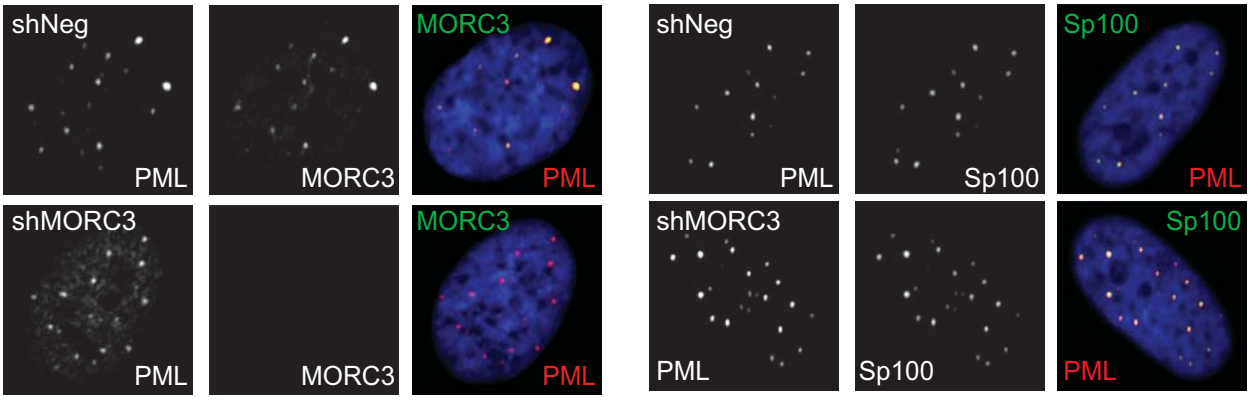
shNeg
PML
MORC3
MORC3
PML
shNeg
PML
Sp100
Sp100
PML
shMORC3
PML
MORC3
MORC3
PML
shMORC3
PML
Sp100
Sp100
PML

C

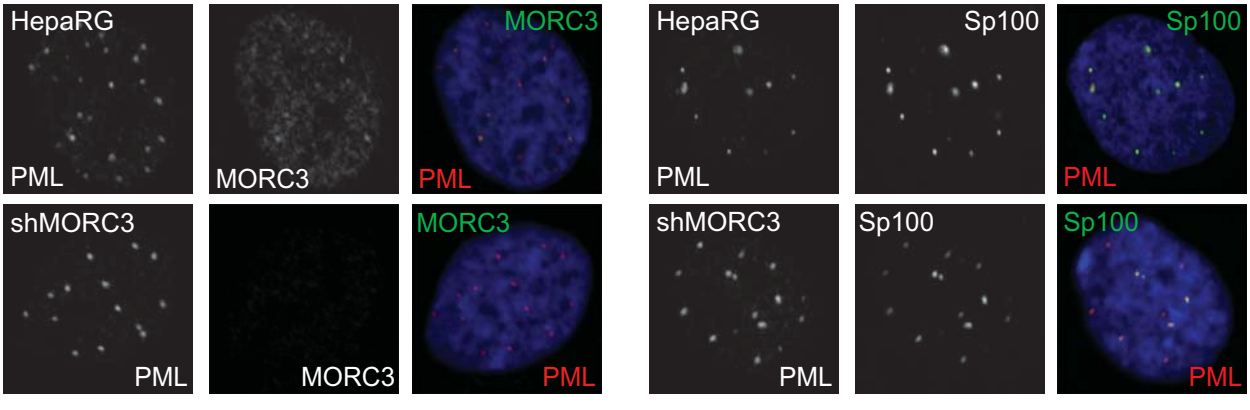
HepaRG
PML
MORC3
MORC3
PML
HepaRG
PML
Sp100
Sp100
PML
shMORC3
PML
MORC3
MORC3
PML
shMORC3
PML
Sp100
Sp100
PML

A

HFT-shMORC3

+ICP4/+PML

HFT-shNEG

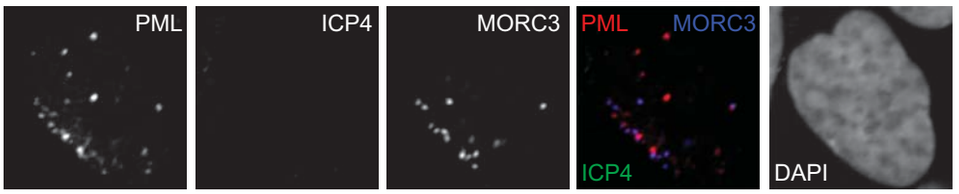

-ICP4/+PML

HFT-shMORC3

+ICP4/-PML

B

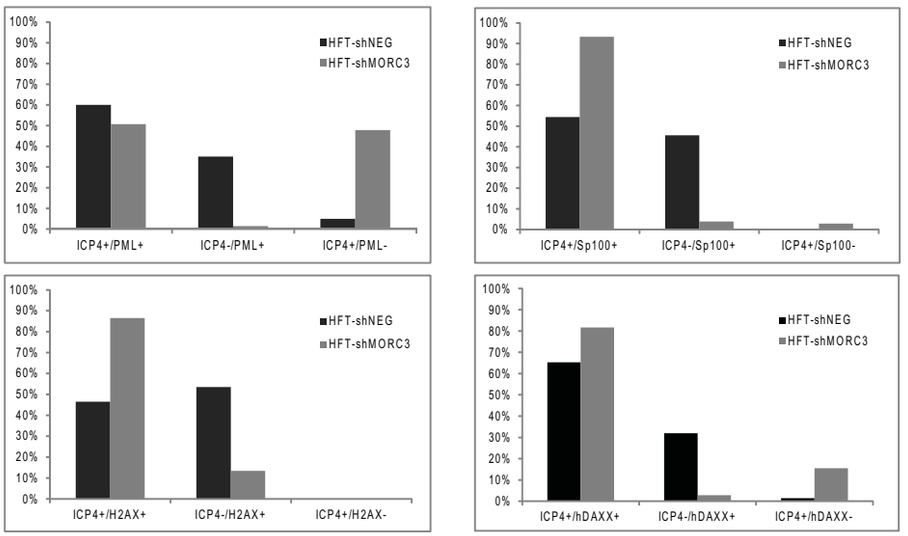

C

HFT-shMORC3
mock

HFT-shMORC3
dl0Y4

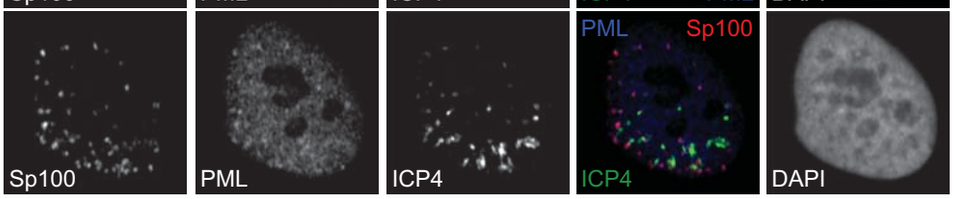

HFT-shNeg
dl0Y4

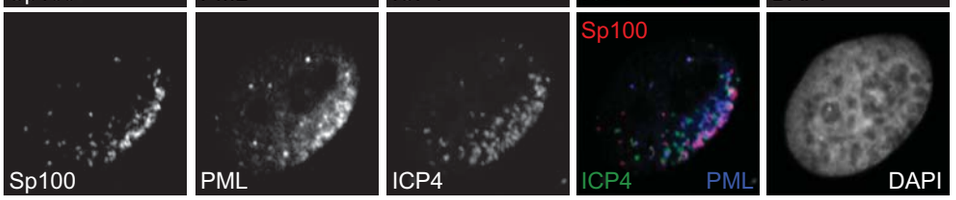

A

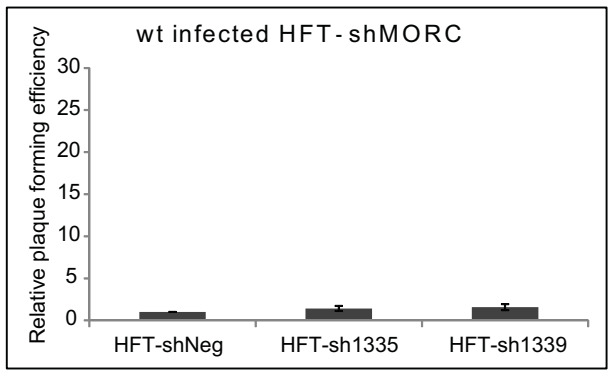
wt infected HFT-shMORC
Relative plaque forming efficiency
30
25
20
15
10
5
0
HFT-shNeg
HFT-sh1335
HFT-sh1339

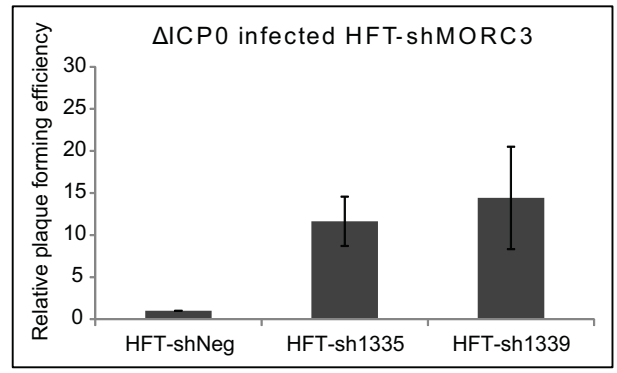
ΔICP0 infected HFT-shMORC3
Relative plaque forming efficiency
30
25
20
15
10
5
0
HFT-shNeg
HFT-sh1335
HFT-sh1339

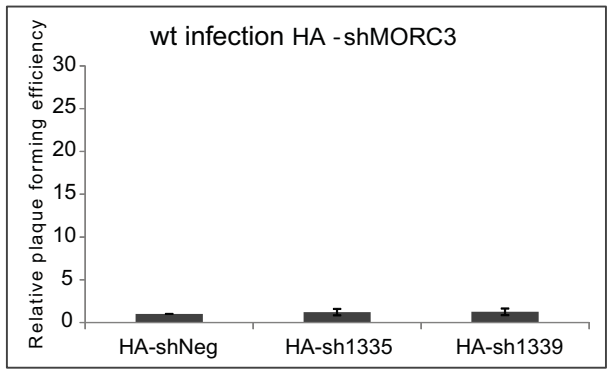
wt infection HA-shMORC3
Relative plaque forming efficiency
30
25
20
15
10
5
0
HA-shNeg
HA-sh1335
HA-sh1339

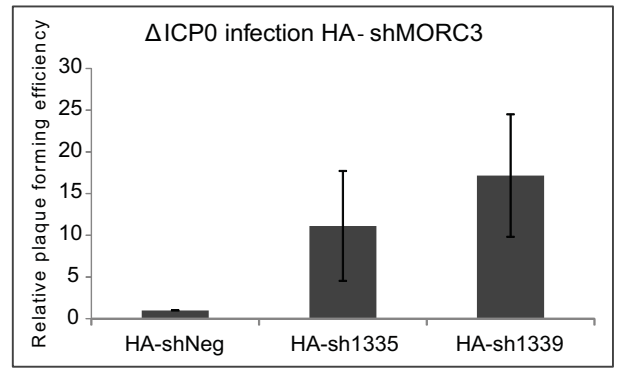
ΔICP0 infection HA-shMORC3
Relative plaque forming efficiency
30
25
20
15
10
5
0
HA-shNeg
HA-sh1335
HA-sh1339

B

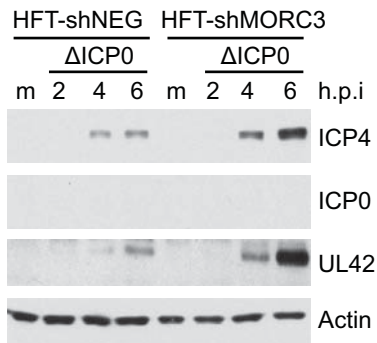
HFT-shNEG
HFT-shMORC3
ΔICP0
ΔICP0
m 2 4 6 m 2 4 6 h.p.i
ICP4
ICP0
UL42
Actin

C

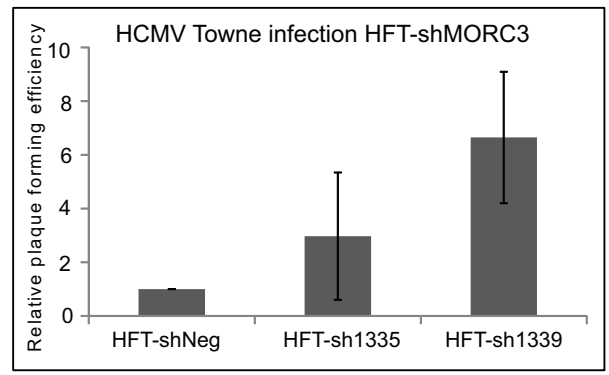
HCMV Towne infection HFT-shMORC3
Relative plaque forming efficiency
10
8
6
4
2
0
HFT-shNeg
HFT-sh1335
HFT-sh1339